

## Light delocalization in a photonic crystal by a fill-factor degeneracy

D. R. Solli<sup>1,\*</sup> and J. M. Hickmann<sup>2</sup>

<sup>1</sup>*Department of Physics, University of California, Berkeley, California 94720-7300, USA*

<sup>2</sup>*Departamento de Física, Universidade Federal de Alagoas, Cidade Universitária, 57072-970, Maceió, AL, Brazil*

(Revised manuscript received 9 June 2006; published 6 November 2006)

We identify an effect wherein the fundamental band gap of a photonic crystal lattice can be suppressed by unexpected mode degeneracy, rendering it completely transparent across two or more bands. We discuss a very simple solid-state analog of these effects based on a mass-spring lattice and show that suppression of the primary photonic band gap is nontrivial and surprising, especially if it simultaneously vanishes for all directions. The lack of a primary band gap in any direction is the opposite of the complete band gap, which is highly coveted in photonic crystal design. Ironically, the complete lack of a band gap also requires special circumstances and may have useful applications.

DOI: [10.1103/PhysRevB.74.195102](https://doi.org/10.1103/PhysRevB.74.195102)

PACS number(s): 42.70.Qs, 41.20.Jb, 42.79.-e

Photonic crystals are the focal point of a great deal of research in modern optics. These wavelength-scale, periodic, dielectric structures offer tantalizing possibilities of controlling light much like crystals control electrons in solid-state physics. The basis for this concept is the existence of a band structure for electromagnetic waves in a periodic dielectric medium, which leads to the possibility of a photonic band gap—a range of frequencies for which there is no propagating mode—analogue to the electronic band gaps of solid-state physics.<sup>1</sup> Because the band structures of photonic crystals depend critically on the lattice geometry, polarization, and the strengths of the constituent dielectric materials,<sup>2</sup> there is tremendous range of possibilities for tailoring and designing photonic crystal structures for a myriad of different applications.

One class of photonic crystals that has received a significant amount of recent attention are two-dimensional (2D) structures, which consist of a periodic plane and a third extruded or nonperiodic dimension.<sup>3,4</sup> These crystals have important practical significance because they offer the possibility of guiding and manipulating light in planar defect circuits<sup>5</sup> and photonic crystal fibers,<sup>6,7</sup> and controlling polarization through their anisotropic band structures.<sup>8,9</sup> Typical 2D photonic crystal lattices include dielectric rods or pipes (tubes) arranged periodically in air, and spaced air holes in a dielectric block. These two-dimensional lattices are often described in terms their air-filling fraction (AFF), the ratio of the air volume in the structure to its total volume. The pipe lattice—a connected array of pipes or tubes—is of particular practical interest. Because each pipe makes tangential contact with its nearest neighbors, the lattice constant  $a$  is equal to the outer diameter of the pipes and the air-filling fraction is determined by the inner diameters of the pipes (as the inner diameter increases, the AFF increases). The interstitial holes between the pipes are all disconnected from one another just as the pipe holes.<sup>6,10</sup> Diagrams of the square and hexagonal lattices of pipes are shown in Fig. 1.

Large AFFs are generally considered important for creating wide, complete photonic band gaps necessary for many photonic crystal applications;<sup>11</sup> however, the performance characteristics of most 2D lattices have not been fully studied over much of the air-filling fraction parameter space for in-plane propagation. As a result, many important questions

concerning the design of photonic-crystal devices remain unanswered, including the effects of noncontiguous regions of the same material. For example, the roles of pipe holes and interstitial holes (between the pipes) in the overall band structure of the pipe lattice have not been thoroughly studied.

In this paper, we present a numerical study of simple square and hexagonal (triangular) lattices of pipes over a range of air-filling fractions from the minima to large values approaching unity. We demonstrate quantitatively how the fundamental band gaps of these structures depend on the air-filling fraction for different dielectrics, and show that their widths and reflectivities are maximized and minimized at particular points in AFF space. We identify an effect wherein the fundamental band gap of a 2D lattice can be suppressed by unexpected mode degeneracy and discuss a very simple solid-state analog of these effects based on a mass-spring lattice. Suppression of the primary photonic band gap is nontrivial and surprising, especially if it simultaneously vanishes for all directions. Band gap suppression, or light delocalization, is stable against disorder, with a band gap gradually opening as disorder is introduced into a finite structure.

We begin our survey with a study of hexagonal and square lattices of a finite number of layers. From an applications point of view, simulations of finite crystals are particularly important because realistic crystals generally consist of a finite number of cells in the direction of propagation. Furthermore, studying finite crystals makes it possible to determine the exponential-attenuation length of the power transmitted by the crystal in the band gap, an important parameter

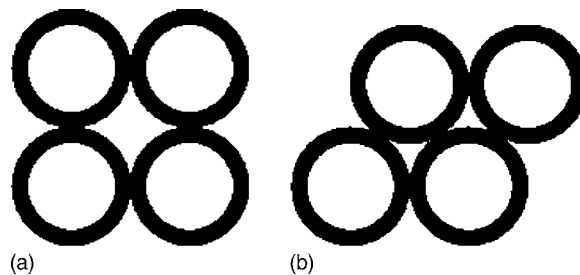


FIG. 1. Schematic diagrams of the square (a) and hexagonal (b) lattices of pipes.

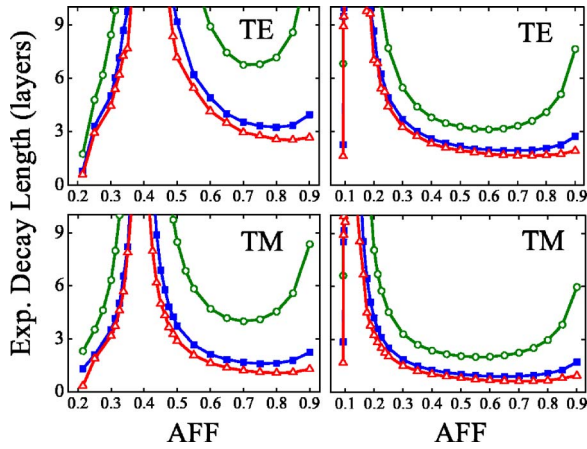


FIG. 2. (Color online) Calculated power exponential attenuation lengths for square (left-hand panels) and hexagonal (right-hand panels) lattices of pipes with  $n=1.61$  (open circles), 2.5 (solid squares), and 3.46 (open triangles) for TE and TM polarizations.

for designing real devices. Using two-dimensional, finite-element, harmonic simulations, we have calculated the power transmitted through lattices—finite in the direction of propagation but infinite in the transverse dimensions—as a function of frequency for different values of the dielectric index of refraction. The sizes of the finite elements were determined by an adaptive algorithm that formed a continuous mesh with finer elements near boundaries and coarser elements away from these regions. Periodic boundary conditions were employed in the periodic plane only in the direction transverse to the propagation. The transmission was calculated for radiation propagating in the  $\Gamma X$  (square lattice) and  $\Gamma M$  (hexagonal lattice) directions, incident on the crystals from air and transmitted into air. We calculated the normalized transmission through the crystal at each frequency using a repetitive loop to run the simulation at regular frequency intervals. To quantify the band gap reflectivity, we determined the transmission through crystals ranging from 10 to 20 layers of pipes (in unit step) for each AFF, and computed the  $1/e$  power exponential-attenuation length by fitting an exponential decay curve to points of minimum transmission in the fundamental band gap.

In Fig. 2, we display the results of these calculations for both TE- and TM-polarized waves (TE,  $\mathbf{E}$ -field perpendicular to periodic plane; TM,  $\mathbf{E}$ -field parallel to periodic plane) for the two lattice geometries and three different refractive-index contrasts. The exponential attenuation length clearly becomes very large—perhaps infinite—over a range of AFFs near 0.4 and 0.14 for the square and hexagonal lattices, respectively.

The primary band gap essentially vanishes at these special air-filling fractions, regardless of the refractive index of the pipes. Because of this unusual property, this effect must rely on some interplay between different regions of the same index of refraction: the pipe holes and the interstitial holes. Simple calculations show that the pipe holes and interstitial holes consume almost identical fractions of the unit-cell area at the air-filling fractions where the band gaps vanish. This suggests that the primary band gap unexpectedly vanishes at

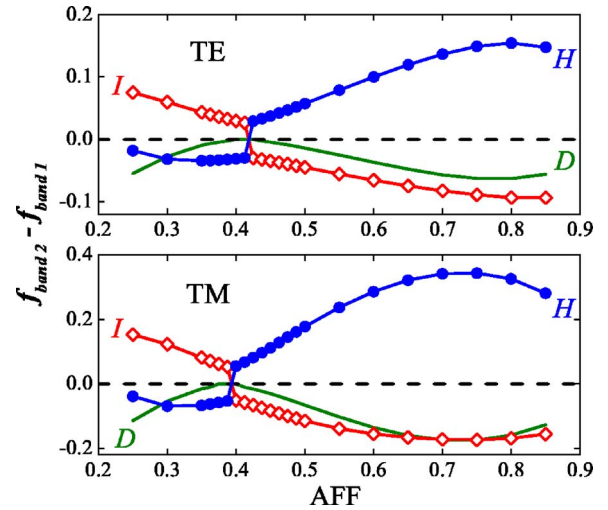


FIG. 3. (Color online) Fill-factor differences between the first two bands of a square lattice of pipes with  $n=1.61$  for TE and TM polarizations.  $D$ ,  $H$ , and  $I$  label the dielectric regions, pipe holes, and interstitial holes, respectively.

these AFFs because the interstitial holes and pipe holes act as equivalent regions for some wave vector in the first two bands. On the other hand, these two regions obviously have different shapes, which explains why the band gaps vanish at AFFs that are slightly lower than predicted by the simple area calculation: since continuity requirements restrict the fields from strongly probing the sharp points of the interstitial holes, the fields must be concentrated more strongly in smaller quasicircular regions. The discrepancy is greater for the hexagonal lattice because the corners of its interstitial holes are sharper compared with those of the square lattice, and for TM modes since their electric fields lie in the periodic plane.

A quantitative approach can be obtained using the so-called fill-factor integrals. The fill factor of a mode over a region  $R$  within the unit cell is the normalized integral of the time-averaged electric energy over that region.<sup>2</sup> For the purposes of our discussion, we define fill factors for the dielectric pipes, pipe holes, and interstitial holes as  $f_D$ ,  $f_H$ , and  $f_I$ , respectively. Since it is energetically favorable to concentrate displacement field in regions of higher dielectric strength, two adjacent bands will be separated by an energy gap if their values of  $f_D$  are different at the edge of the Brillouin zone;<sup>2</sup> however, redistribution of fields between the interstitial holes and the pipe holes does not in itself generate an energy gap.

In Fig. 3 we show the changes in  $f_D$ ,  $f_H$ , and  $f_I$  across the  $X$ -point edges of the first two bands in the square lattice of pipes as a function of the air-filling fraction. We computed the fill factors by averaging the integrals over 10 unit cells along the direction of propagation in a lattice of 20 layers. The change in dielectric fill factor has polarization-dependent local extrema at the special AFFs where the band gaps disappear and at higher air-filling fractions where the power attenuation lengths have local minima. Notice that at low air-filling fractions,  $f_I$  increases and  $f_H$  decreases from the first band to the second, whereas, the opposite is true for

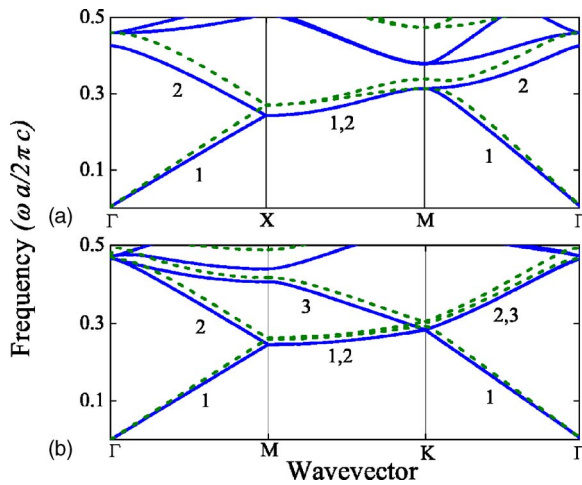


FIG. 4. (Color online) TE (solid curves) and TM (dashed curves) band diagrams (TE labeled by number) of square (a) and hexagonal (b) lattices of pipes. (TE, TM) AFFs: (a) (0.415, 0.388); (b) (0.14, 0.12).

the high AFFs. In the low AFF regime, the magnitude of the change in  $f_l$  is larger than that of  $f_H$ , but at high air-filling fractions,  $f_H$  dominates.

These features indicate that at low AFF, the fundamental band gaps are primarily due to a displacement-field shift from the dielectric regions and pipe holes in the first band to the *interstitial* holes in the second band, whereas, at high AFF they are mostly due to a field shift from the dielectric regions and interstitial holes in the first band to the *pipe* holes in the second band. Because of continuity restrictions, the fundamental mode cannot be completely confined to the dielectric regions, but must also occupy either the pipe holes or the interstitial holes. The magnitudes of the fill-factor changes illustrates that it is energetically favorable for the fundamental mode to choose the pipe holes at low AFF and the interstitial holes at high AFF. The transition between these two regimes are the special air-filling fractions where the band gaps vanish.

In order to study the complete band structures of the square and hexagonal pipe lattices, we also performed band calculations spanning the perimeters of their irreducible Brillouin zones. These band structures were calculated by determining the eigenmodes and corresponding eigenfrequencies of a single unit cell of the particular lattice with periodic boundary conditions. A repetitive loop was used to repetitively run the simulation for wave vectors spanning the Brillouin zone at regular intervals. In Fig. 4, we show the band maps for the square and hexagonal lattices of pipes at the air-filling fractions where the band gaps were seen to vanish. Notice that for both lattice types, there is essentially no band gap between the first two TE modes for any direction of propagation at the special air-filling fractions. Interestingly, for the hexagonal lattice, the *K* point is actually a triple point for TE waves, an intersection between the first three bands. On the other hand, the TM gap does not completely disappear for all directions in either pipe lattice. It vanishes for the  $\Gamma X$  direction, but does not completely disappear for other directions of propagation likely because continuity restric-

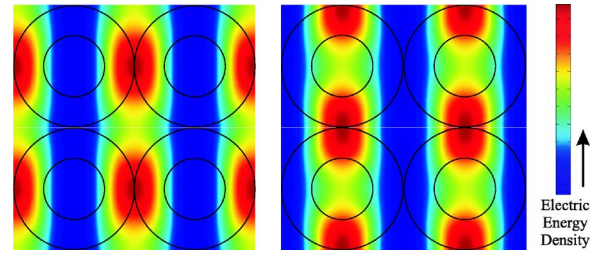


FIG. 5. (Color online) The time-averaged electric energy density distributions (arbitrary units) for TE waves in band 1 (left-hand plot) and band 2 (right-hand plot) at the X point in a square lattice of pipes with AFF of 0.415 and  $n=2.5$ . The black circles delineate the outside and inside perimeters of the pipe walls.

tions force a change in the dielectric fill factor between the first two modes. In order to illustrate these unexpected mode degeneracies with an example, we have plotted in Fig. 5 the time-averaged electric energy distributions for TE waves in bands 1 and 2 at the X point in a square lattice of pipes with the special air-filling fraction (refractive index  $n=2.5$ ). From these plots, it is clear that the pipe holes and the interstitial holes act as equivalent regions for TE waves at the X point in this crystal.

Finally, we have also performed calculations to characterize the complete band gaps of the pipe lattices for other air-filling fractions. Evidently, the primary band gap does not simultaneously cover all directions for TE waves in either the square or hexagonal lattices for any index contrast and AFF. On the other hand, there are complete, primary TM band gaps in both lattice types with sufficient dielectric strengths ( $n \geq 1.5$  for the hexagonal lattice;  $n \geq 2.5$  for the square lattice). In Fig. 6, we plot the complete TM band gap widths as functions of the AFF for three different dielectrics. The complete band gap widths are maximized at index-independent values of the air-filling fraction, which increase with the dielectric strength; however, these extrema do not coincide precisely with the minimum attenuation lengths displayed in Fig. 2.

The existence of AFFs that maximize the widths and reflectivities of the band gaps can also be understood in terms

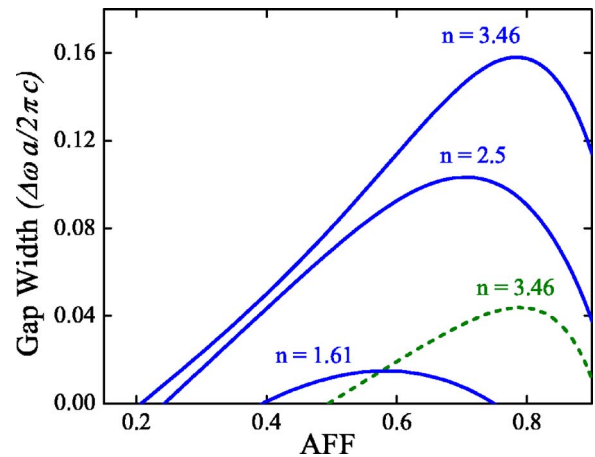


FIG. 6. (Color online) Complete TM band gap widths in square (dashed curve) and hexagonal lattices (solid curves) of pipes.

of the fill factor. The size of the band gap increases if there is a greater discrepancy between the dielectric fill factors at the edge of the Brillouin zone. This discrepancy can only increase up to a certain point—as the AFF is increased beyond this point, more of the field must spill out of the thin dielectric regions into the air regions even in the dielectric band. This leads to a smaller difference between the dielectric fill factors of the first two bands. Thus, contrary to what is often implied in the literature, the widths and reflectivities of these band gaps do not continually increase at high air-filling fractions, but reach maximum values that depend on the index contrast.

An analogy with solid state physics clarifies the connection between band gap suppression and fill-factor degeneracy. It is well known that the frequency gap between the optical and acoustical phonon dispersion branches of a linear diatomic crystal at the Brillouin zone edge is given by  $\Delta\omega = \sqrt{2k/m_2} - \sqrt{2k/m_1}$ , where  $m_1$  and  $m_2$  are the masses of two atomic species ( $m_1 > m_2$ ) and  $k$  characterizes the strength of the coupling between them.<sup>12</sup> Clearly, if we let  $m_1 \rightarrow m_2$ , then the gap between the branches vanishes. In the photonic crystal case, the quantity analogous to the atomic mass is the dielectric fill factor  $f_D$  since  $\Delta f_D$  at the edge of the Brillouin zone determines the size of the frequency gap. In the simple diatomic case, the band gap vanishes if the two masses are equal; in the photonic crystal case the primary band gap can be suppressed by the crystal geometry even if the refractive index contrast is large because the fill factor depends on both of these properties. This phenomenon is very general and can result in the unexpected suppression of a band gap even when the modal distributions between two adjacent bands are quite different, as long as the dielectric fill factors at that point happen to be the same.

Interestingly, gap-suppressed crystals are affected by disorder differently from normal photonic crystals. We have performed 2D numerical simulations of finite pipe lattices with disorder by adding a random component to the inner radius of the pipes, but holding the lattice constant fixed. As the amplitude of the disorder was increased from zero, we observed markedly different transmission properties depend-

ing on the average air-filling fraction. We found that the effect of band gap suppression persists in finite, disordered structures, with the band gap gradually opening as the disorder increases. Furthermore, for some range of air-filling fractions around the gap-suppressed value, this unusual behavior occurs: introduction of disorder gradually increases the opacity of the structure. This behavior contrasts with what is known to occur when disorder is introduced into a normal finite photonic band gap crystal. On the other hand, outside of this AFF range, the normal trend is observed. Thus, introduction of disorder either increases or decreases the size of the photonic band gap depending on the air-filling fraction.

In conclusion, we have characterized the square and hexagonal lattices of pipes over a large range of air-filling fractions. Our simulations have demonstrated the existence of unexpected special points and band gap trends, which may be extremely useful in optimizing the design of photonic crystal devices. As we have shown, fill-factor degeneracies can result in the complete destruction of the primary band gap. In some sense, this is the opposite of the coveted complete band gap spanning all in-plane directions;<sup>13</sup> ironically, the complete lack of a primary band gap in a periodic structure with significant index contrast can be achieved but is also apparently somewhat difficult. Band gap suppression also exists in three-dimensional photonic lattices, with the fill factors reinterpreted as volume integrals. One of the interesting things about photonic crystals is not just the existence of the band gap, but that an ordered array of scatterers can be transparent due to constructive interference. Thus, photonic band gap suppression is surprising because it means that an array of scatterers is completely transparent to all frequencies across two distinct bands. These effects may have application in the design of broad-band photonic crystal waveplates, which require structures that are both birefringent and transparent.<sup>9</sup> Finally, these concepts may be also useful for the construction of bistable devices based on nonlinear photonic crystals.

One of the authors (J.M.H.) thanks the support from Instituto do Milênio de Informação Quântica, CAPES, CNPq, FAPEAL, PADCT, CT-INFRA.

\*Present address: Department of Electrical Engineering, University of California, Los Angeles, CA 90095.

<sup>1</sup>E. Yablonovitch, *Phys. Rev. Lett.* **58**, 2059 (1987).

<sup>2</sup>J. D. Joannopoulos, R. D. Meade, and J. Winn, *Photonic Crystals: Molding the Flow of Light* (Princeton University Press, Princeton, NJ, 1995), Chap 5.

<sup>3</sup>S. L. McCall, P. M. Platzman, R. Dalichaouch, D. Smith, and S. Schultz, *Phys. Rev. Lett.* **67**, 2017 (1991).

<sup>4</sup>E. Chow, S. Y. Lin, S. G. Johnson, P. R. Villeneuve, J. D. Joannopoulos, J. R. Wendt, G. A. Vawter, W. Zubrzycki, H. Hou, and A. Alleman, *Nature (London)* **407**, 983 (2000).

<sup>5</sup>J. D. Joannopoulos, P. R. Villeneuve, and S. H. Fan, *Nature (London)* **387**, 830 (1997).

<sup>6</sup>R. F. Cregan, B. J. Mangan, J. C. Knight, T. A. Birks, P. St. J. Russell, P. J. Roberts, and D. C. Allan, *Science* **285**, 1537

(1999).

<sup>7</sup>P. Russell, *Science* **299**, 358 (2003).

<sup>8</sup>D. R. Solli, C. F. McCormick, R. Y. Chiao, and J. M. Hickmann, *Opt. Photonics News* **2003**, 35 (2003).

<sup>9</sup>For a review of polarization control using photonic crystals see D. R. Solli and J. M. Hickmann, *J. Phys. D* **37**, R263 (2004).

<sup>10</sup>J. Broeng, S. E. Barkou, A. Bjarklev, J. C. Knight, T. A. Birks, and P. S. Russell, *Opt. Commun.* **156**, 240 (1998).

<sup>11</sup>C. M. Smith, N. Venkataraman, M. T. Gallagher, D. Muller, J. A. West, N. F. Borrelli, D. C. Allan, and K. W. Koch, *Nature (London)* **424**, 657 (2003).

<sup>12</sup>C. Kittel, *Introduction to Solid State Physics* (Wiley, New York, 1996), Chap 4.

<sup>13</sup>R. D. Meade, K. D. Brommer, A. M. Rappe, and J. D. Joannopoulos, *Appl. Phys. Lett.* **61**, 495 (1992).